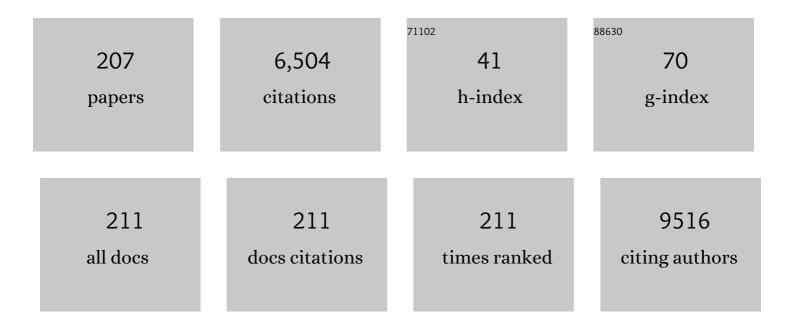
Nikolaos Boukos

List of Publications by Year in descending order

Source: https://exaly.com/author-pdf/1217172/publications.pdf Version: 2024-02-01



#	Article	IF	CITATIONS
1	Study of the photoluminescence of N-doped, Carbon Dot-based nanocomposite materials from citric acid and urea. Functional Materials Letters, 2022, 15, .	1.2	1
2	Bimetallic gold-platinum nanoparticles as a drug delivery system coated with a new drug to target glioblastoma. Colloids and Surfaces B: Biointerfaces, 2022, 214, 112463.	5.0	13
3	Effect of processing temperature on growing bamboo-like carbon nanotubes by chemical vapor deposition. Materials Today Chemistry, 2021, 19, 100388.	3.5	6
4	Low-Cost Electrodeposition of Size-Tunable Single-Crystal ZnO Nanorods. Fibers, 2021, 9, 38.	4.0	6
5	A hyperbranched polymer synthetic strategy for the efficient fixation of metal species within nanoporous structures: Application in automotive catalysis. Chemical Engineering Journal, 2021, 421, 129496.	12.7	9
6	Visible Light Trapping against Charge Recombination in FeOx–TiO2 Photonic Crystal Photocatalysts. Materials, 2021, 14, 7117.	2.9	4
7	Heterostructured CoOx–TiO2 Mesoporous/Photonic Crystal Bilayer Films for Enhanced Visible-Light Harvesting and Photocatalysis. Materials, 2020, 13, 4305.	2.9	7
8	Modified magnetic core-shell mesoporous silica nano-formulations with encapsulated quercetin exhibit anti-amyloid and antioxidant activity. Journal of Inorganic Biochemistry, 2020, 213, 111271.	3.5	22
9	Monitoring the multiphasic evolution of bismuth telluride nanoplatelets. CrystEngComm, 2020, 22, 7918-7928.	2.6	5
10	On the selective oxidation of H2S by heavy loaded Nanoparticles Embedded in Mesoporous Matrix (NEMMs). Applied Catalysis B: Environmental, 2020, 278, 119338.	20.2	13
11	Photocatalytic H2 Evolution, CO2 Reduction, and NOx Oxidation by Highly Exfoliated g-C3N4. Catalysts, 2020, 10, 1147.	3.5	19
12	Boosting visible light harvesting and charge separation in surface modified TiO ₂ photonic crystal catalysts with CoO _x nanoclusters. Materials Advances, 2020, 1, 2310-2322.	5.4	13
13	Novel Isatin Thiosemicarbazone Derivatives as Potent Inhibitors of β-Amyloid Peptide Aggregation and Toxicity. ACS Chemical Neuroscience, 2020, 11, 2266-2276.	3.5	15
14	Magnetic fluid hyperthermia simulations in evaluation of SAR calculation methods. Physica Medica, 2020, 71, 39-52.	0.7	24
15	Patterned carbon dot-based thin films for solid-state devices. Nanoscale, 2020, 12, 10254-10264.	5.6	13
16	Graphene Quantum Dot-TiO2 Photonic Crystal Films for Photocatalytic Applications. Nanomaterials, 2020, 10, 2566.	4.1	11
17	Advanced Photocatalysts Based on Reduced Nanographene Oxide–TiO2 Photonic Crystal Films. Materials, 2019, 12, 2518.	2.9	10
18	Synthesis, characterization and evaluation of multi sensitive nanocarriers by using the layer by layer method. Journal of Drug Delivery Science and Technology, 2019, 53, 101142.	3.0	4

#	Article	IF	CITATIONS
19	Molecular/Nanostructured Functional Metal Oxide Stacks for Nanoscale Nanosecond Information Storage. Advanced Functional Materials, 2019, 29, 1902642.	14.9	2
20	Gold nanoparticle decorated pH-sensitive polymeric nanocontainers as a potential theranostic agent. Colloids and Surfaces B: Biointerfaces, 2019, 183, 110420.	5.0	26
21	Spin-Crossover Phenomenon in Microcrystals and Nanoparticles of a [Fe(2-mpz) ₂ Ni(CN) ₄] Two-Dimensional Hofmann-Type Polymer: A Detailed Nano-Topographic Study. Inorganic Chemistry, 2019, 58, 13733-13736.	4.0	18
22	Efficient photocatalytic water-splitting performance by ternary CdS/Pt-N-TiO2 and CdS/Pt-N,F-TiO2: Interplay between CdS photo corrosion and TiO2-dopping. Applied Catalysis B: Environmental, 2019, 254, 194-205.	20.2	86
23	Nanographene oxide–TiO ₂ photonic films as plasmon-free substrates for surface-enhanced Raman scattering. Nanoscale, 2019, 11, 21542-21553.	5.6	26
24	Effects of Precursor Concentration in Solvent and Nanomaterials Room Temperature Aging on the Growth Morphology and Surface Characteristics of Ni–NiO Nanocatalysts Produced by Dendrites Combustion during SCS. Applied Sciences (Switzerland), 2019, 9, 4925.	2.5	10
25	Titania photonic crystal photocatalysts functionalized by graphene oxide nanocolloids. Applied Catalysis B: Environmental, 2019, 240, 277-290.	20.2	43
26	Photocatalytic properties of copper—Modified core-shell titania nanocomposites. Journal of Photochemistry and Photobiology A: Chemistry, 2019, 370, 145-155.	3.9	25
27	Two completely different biomimetic reactions mediated by the same matrix producing inorganic/organic/inorganic hybrid nanoparticles. Nano Structures Nano Objects, 2018, 14, 138-148.	3.5	10
28	Preparation of CuO/SBA-15 catalyst by the modified ammonia driven deposition precipitation method with a high thermal stability and an efficient automotive CO and hydrocarbons conversion. Applied Catalysis B: Environmental, 2018, 223, 103-115.	20.2	30
29	Enhanced NO 2 abatement by alkaline-earth modified g-C 3 N 4 nanocomposites for efficient air purification. Applied Surface Science, 2018, 430, 225-233.	6.1	33
30	Coalescence of Cluster Beam Generated Subâ€⊋ nm Bare Au Nanoparticles and Analysis of Au Film Growth Parameters. Annalen Der Physik, 2018, 530, 1700256.	2.4	2
31	Facile MoS2 Growth on Reduced Graphene-Oxide via Liquid Phase Method. Frontiers in Materials, 2018, 5, .	2.4	5
32	Noncovalent Grafting of a Dy ^{III} ₂ Single-Molecule Magnet onto Chemically Modified Multiwalled Carbon Nanotubes. Inorganic Chemistry, 2018, 57, 6391-6400.	4.0	8
33	Chemical vs thermal exfoliation of g-C3N4 for NOx removal under visible light irradiation. Applied Catalysis B: Environmental, 2018, 239, 16-26.	20.2	185
34	Polaron freezing and the quantum liquid-crystal phase in the ferromagnetic metallic La0.67Ca0.33MnO3. Npj Quantum Materials, 2018, 3, .	5.2	8
35	Synthesis of hafnium nanoparticles and hafnium nanoparticle films by gas condensation and energetic deposition. Beilstein Journal of Nanotechnology, 2018, 9, 1868-1880.	2.8	6
36	Tailoring the energy band gap and edges' potentials of g-C 3 N 4 /TiO 2 composite photocatalysts for NO x removal. Chemical Engineering Journal, 2017, 310, 571-580.	12.7	325

#	Article	IF	CITATIONS
37	Self-propagating solar light reduction of graphite oxide in water. Applied Surface Science, 2017, 391, 601-608.	6.1	25
38	Resistive memory multilayer structure with self-rectifying and forming free properties along with their modification by adding a hafnium nanoparticle midlayer. Journal of Vacuum Science and Technology A: Vacuum, Surfaces and Films, 2017, 35, .	2.1	3
39	Novel â€~Pickering' modified TiO 2 photocatalysts with high De-NOx efficiency. Catalysis Today, 2017, 287, 45-51.	4.4	11
40	Coexistence of bipolar and threshold resistive switching in TiO ₂ based structure with embedded hafnium nanoparticles. Journal Physics D: Applied Physics, 2017, 50, 045103.	2.8	11
41	An integrated bacterial system for the discovery of chemical rescuers of disease-associated protein misfolding. Nature Biomedical Engineering, 2017, 1, 838-852.	22.5	22
42	Improved Stability of Polymer Solar Cells in Ambient Air via Atomic Layer Deposition of Ultrathin Dielectric Layers. Advanced Materials Interfaces, 2017, 4, 1700231.	3.7	8
43	Graphene-based materials via benzidine-assisted exfoliation and reduction of graphite oxide and their electrochemical properties. Applied Surface Science, 2017, 392, 244-255.	6.1	32
44	Graphene by one-step chemical vapor deposition from ferrocene vapors: Properties and electrochemical evaluation. Journal of Applied Physics, 2016, 119, .	2.5	13
45	Hyperbranched polyethyleneimine towards the development of homogeneous and highly porous CuO–CeO2–SiO2 catalytic materials. Chemical Engineering Journal, 2016, 300, 343-357.	12.7	14
46	Unexpected orbital magnetism in Bi-rich Bi2Se3 nanoplatelets. NPG Asia Materials, 2016, 8, e271-e271.	7.9	9
47	Thermochromic performance of Mg-doped VO2 thin films on functional substrates for glazing applications. Solar Energy Materials and Solar Cells, 2016, 157, 1004-1010.	6.2	60
48	Metal loaded nanoporous silicas with tailor-made properties through hyperbranched polymer assisted templating approaches. Microporous and Mesoporous Materials, 2016, 235, 107-119.	4.4	11
49	Sustained release profile of quatro stimuli nanocontainers as a multi sensitive vehicle exploiting cancer characteristics. Colloids and Surfaces B: Biointerfaces, 2016, 148, 95-103.	5.0	22
50	Experimental investigation of metallic thin film modification of nickel substrates for chemical vapor deposition growth of single layer graphene at low temperature. Applied Surface Science, 2016, 385, 554-561.	6.1	12
51	Efficient CO oxidation in an ionic liquid-modified, Au nanoparticle-loaded membrane contactor. Chemical Engineering Journal, 2016, 305, 79-91.	12.7	15
52	Biomimetic synthesis of ribbon-like hydroxyapatite employing poly(l -arginine). Materials Science and Engineering C, 2016, 58, 1225-1231.	7.3	19
53	TiO2/graphene composite photocatalysts for NOx removal: A comparison of surfactant-stabilized graphene and reduced graphene oxide. Applied Catalysis B: Environmental, 2016, 180, 637-647.	20.2	199
54	Water Coordination, Proton Mobility, and Lewis Acidity in HY Nanozeolites: A High-Temperature ¹ H and ²⁷ Al NMR Study. Journal of Physical Chemistry C, 2015, 119, 3428-3438.	3.1	12

#	Article	IF	CITATIONS
55	Synthesis, structure and photoluminescence of (PLAGH)2[ZnCl4] and comparative analysis of photoluminescence properties with tris(2,2′-bipyridine)ruthenium(II). Materials Research Bulletin, 2015, 70, 951-957.	5.2	8
56	Eco-efficient TiO2 modification for air pollutants oxidation. Applied Catalysis B: Environmental, 2015, 176-177, 578-585.	20.2	28
57	Reducing the layer number of AB stacked multilayer graphene grown on nickel by annealing at low temperature. Nanotechnology, 2015, 26, 405603.	2.6	6
58	Decoration of crumpled rGO sheets with Ag nanoparticles by spray pyrolysis. Applied Surface Science, 2015, 358, 84-90.	6.1	11
59	Non-activated high surface area expanded graphite oxide for supercapacitors. Applied Surface Science, 2015, 358, 110-121.	6.1	42
60	Effect of hydrothermal reaction time and alkaline conditions on the electrochemical properties of reduced graphene oxide. Applied Surface Science, 2015, 358, 100-109.	6.1	47
61	Solvothermal synthesis and photocatalytic performance of Mn 4+ -doped anatase nanoplates with exposed {0 0 1} facets. Applied Catalysis B: Environmental, 2015, 162, 27-33.	20.2	54
62	A Novel Method for the Growth of Cu2O/ZnO Heterojunctions. Energy Procedia, 2014, 60, 37-42.	1.8	6
63	One-step, in situ growth of unmodified graphene – magnetic nanostructured composites. Carbon, 2014, 66, 467-475.	10.3	23
64	pH- and thermo-responsive microcontainers as potential drug delivery systems: Morphological characteristic, release and cytotoxicity studies. Materials Science and Engineering C, 2014, 37, 271-277.	7.3	25
65	Development of Multiple Stimuli Responsive Magnetic Polymer Nanocontainers as Efficient Drug Delivery Systems. Macromolecular Bioscience, 2014, 14, 131-141.	4.1	28
66	Dynamic in vivo imaging of dual-triggered microspheres for sustained release applications: Synthesis, characterization and cytotoxicity study. International Journal of Pharmaceutics, 2014, 461, 54-63.	5.2	23
67	A high-performance adsorbent for hydrogen sulfide removal. Microporous and Mesoporous Materials, 2014, 190, 152-155.	4.4	63
68	Solvothermal synthesis and photocatalytic performance of Mg2+-doped anatase nanocrystals with exposed {001} facets. Catalysis Today, 2014, 230, 125-130.	4.4	19
69	TiO2 functionalization for efficient NOx removal in photoactive cement. Applied Surface Science, 2014, 319, 29-36.	6.1	44
70	Atomicâ€Layerâ€Deposited Aluminum and Zirconium Oxides for Surface Passivation of TiO ₂ in Highâ€Efficiency Organic Photovoltaics. Advanced Energy Materials, 2014, 4, 1400214.	19.5	52
71	Photoluminescence properties and comparative analysis of the new compound of Zn(II) with piridoxalaminoguanidine and Ru(II) bipyridine complex. , 2014, , .		0
72	Hollow microspheres based on – Folic acid modified – Hydroxypropyl Cellulose and synthetic multi-responsive bio-copolymer for targeted cancer therapy: Controlled release of daunorubicin, in vitro and in vivo studies. Journal of Colloid and Interface Science, 2014, 435, 171-181.	9.4	29

#	Article	IF	CITATIONS
73	Decoration of TiO2 anatase nanoplates with silver nanoparticles on the {101} crystal facets and their photocatalytic behaviour. Applied Catalysis B: Environmental, 2014, 158-159, 91-95.	20.2	61
74	Influence of the Oxygen Substoichiometry and of the Hydrogen Incorporation on the Electronic Band Structure of Amorphous Tungsten Oxide Films. Journal of Physical Chemistry C, 2014, 118, 12632-12641.	3.1	46
75	A new approach for the one-step synthesis of bioactive PS vs. PMMA silica hybrid microspheres as potential drug delivery systems. Colloids and Surfaces B: Biointerfaces, 2014, 117, 322-329.	5.0	13
76	Reduced graphene oxide/iron carbide nanocomposites for magnetic and supercapacitor applications. Journal of Alloys and Compounds, 2014, 590, 102-109.	5.5	72
77	Deterioration of exchange bias in CoO-Co bilayers by the roughness of the ZnO substrates. EPJ Web of Conferences, 2014, 75, 05011.	0.3	0
78	Efficient removal of hexavalent chromium from aqueous solutions using autohydrolyzed Scots Pine (Pinus Sylvestris) sawdust as adsorbent. International Journal of Environmental Science and Technology, 2013, 10, 1337-1348.	3.5	11
79	Nanostructuring the Surface of Dual Responsive Hollow Polymer Microspheres for Versatile Utilization in Nanomedicine-Related Applications. Langmuir, 2013, 29, 9562-9572.	3.5	26
80	Comparative study of LbL and crosslinked pH sensitive PEGylated LbL microspheres: Synthesis, characterization and biological evaluation. Colloids and Surfaces B: Biointerfaces, 2013, 104, 91-98.	5.0	14
81	Microspheres as therapeutic delivery agents: synthesis and biological evaluation of pH responsiveness. Journal of Materials Chemistry B, 2013, 1, 194-203.	5.8	37
82	N and N,S-doped TiO2 photocatalysts and their activity in NOx oxidation. Catalysis Today, 2013, 209, 41-46.	4.4	54
83	Inorganic–organic core–shell titania nanoparticles for efficient visible light activated photocatalysis. Applied Catalysis B: Environmental, 2013, 130-131, 14-24.	20.2	87
84	Electrical conductivity studies of anatase TiO2 with dominant highly reactive {001} facets. Journal of Alloys and Compounds, 2013, 548, 194-200.	5.5	48
85	A novel hybrid sol–gel method for the synthesis of highly porous silica employing hyperbranched poly(ethyleneimine) as a reactive template. Microporous and Mesoporous Materials, 2013, 175, 59-66.	4.4	24
86	<i>In Situ</i> Deposition and Characterization of MoS ₂ Nanolayers on Carbon Nanofibers and Nanotubes. Journal of Physical Chemistry C, 2013, 117, 10135-10142.	3.1	35
87	Laser printing and characterization of semiconducting polymers for organic electronics. Applied Physics A: Materials Science and Processing, 2013, 110, 559-563.	2.3	20
88	Tuning the photocatalytic selectivity of TiO2 anatase nanoplates by altering the exposed crystal facets content. Applied Catalysis B: Environmental, 2013, 142-143, 761-768.	20.2	66
89	Synthesis, structure and photoluminescence properties of copper(II) and cobalt(III) complexes with pyridoxalaminoguanidine. Optical Materials, 2013, 35, 2728-2735.	3.6	13
90	Effect of the Oxygen Sub-Stoichiometry and of Hydrogen Insertion on the Formation of Intermediate Bands within the Gap of Disordered Molybdenum Oxide Films. Journal of Physical Chemistry C, 2013, 117, 18013-18020.	3.1	40

#	Article	IF	CITATIONS
91	One-Step Synthesis of TiO _{2} /Perlite Composites by Flame Spray Pyrolysis and Their Photocatalytic Behavior. International Journal of Photoenergy, 2013, 2013, 1-8.	2.5	17
92	Forming-free resistive switching memories based on titanium-oxide nanoparticles fabricated at room temperature. Applied Physics Letters, 2013, 102, 022909.	3.3	31
93	Study of TiO2 anatase nano and microstructures with dominant {001} facets for NO oxidation. Environmental Science and Pollution Research, 2012, 19, 3719-3726.	5.3	41
94	Resistive switching memory using titanium-oxide nanoparticle films. , 2012, , .		0
95	Preparation and Characterization of Polyindole–Iron Oxide Composite Polymer Electrolyte Containing LiClO ₄ . Polymer-Plastics Technology and Engineering, 2012, 51, 225-230.	1.9	34
96	Polysaccharides as a source of advanced materials: Cellulose hollow microspheres for drug delivery in cancer therapy. Journal of Colloid and Interface Science, 2012, 384, 198-206.	9.4	39
97	Zinc related defects in ZnO nanorods. Physica Status Solidi (B): Basic Research, 2012, 249, 560-563.	1.5	4
98	Multiâ€responsive polymeric microcontainers for potential biomedical applications: synthesis and functionality evaluation. Polymer International, 2012, 61, 888-894.	3.1	20
99	Nanodesigned magnetic polymer containers for dual stimuli actuated drug controlled release and magnetic hyperthermia mediation. Journal of Materials Chemistry, 2012, 22, 13451.	6.7	55
100	Novel PEGylated pH-sensitive polymeric hollow microspheres. Materials Letters, 2012, 67, 180-183.	2.6	12
101	Sensitizer activated solar cells based on self-organized TiO2 nanotubes. Microelectronic Engineering, 2012, 90, 62-65.	2.4	13
102	Zinc vacancies and interstitials in ZnO nanorods. Thin Solid Films, 2012, 520, 4654-4657.	1.8	8
103	Polyindole–CuO composite polymer electrolyte containing LiClO4 for lithium ion polymer batteries. Polymer Bulletin, 2012, 68, 181-196.	3.3	32
104	Sacrificial Template-Directed Fabrication of Superparamagnetic Polymer Microcontainers for pH-Activated Controlled Release of Daunorubicin. Langmuir, 2011, 27, 8478-8485.	3.5	32
105	Size control of Ag nanoparticles for SERS sensing applications. Procedia Engineering, 2011, 25, 280-283.	1.2	7
106	A Solid-State Hybrid Solar Cell Made of nc-TiO ₂ , CdS Quantum Dots, and P3HT with 2-Amino-1-methylbenzimidazole as an Interface Modifier. Journal of Physical Chemistry C, 2011, 115, 10911-10916.	3.1	34
107	Controlling the Formation of Hydroxyapatite Nanorods with Dendrimers. Journal of the American Ceramic Society, 2011, 94, 2023-2029.	3.8	52
108	Influence of the composition of Fe2O3/Al2O3 catalysts on the rate of production and quality of carbon nanotubes. Materials Chemistry and Physics, 2011, 128, 96-108.	4.0	20

#	Article	IF	CITATIONS
109	Thermal Aging Behavior of Pt-only TWC Converters Under Simulated Exhaust Conditions: Effect of Rare Earths (CeO2, La2O3) and Alkali (Na) Modifiers. Topics in Catalysis, 2011, 54, 1124-1134.	2.8	27
110	ZnO nanoparticles produced by novel reactive physical deposition process. Applied Surface Science, 2011, 257, 5366-5369.	6.1	11
111	Synergistic structural and surface promotion of monometallic (Pt) TWCs: Effectiveness and thermal aging tolerance. Applied Catalysis B: Environmental, 2011, 106, 228-228.	20.2	13
112	Synthesis and Characterization of Polyindole–NiO-Based Composite Polymer Electrolyte with LiClO ₄ . International Journal of Polymeric Materials and Polymeric Biomaterials, 2011, 60, 877-892.	3.4	32
113	One Pot Synthesis and Characterization of Ultra Fine CeO ₂ and Cu/CeO ₂ Nanoparticles. Application for Low Temperature CO Oxidation. Journal of Nanoscience and Nanotechnology, 2011, 11, 8593-8598.	0.9	11
114	Decoration of Carbon Nanotubes with CoO and Co Nanoparticles. Journal of Nanomaterials, 2011, 2011, 1-9.	2.7	9
115	Preparation and characterization of polyindole–ZnO composite polymer electrolyte with LiClO4. Ionics, 2010, 16, 839-848.	2.4	34
116	A Closer Look Inside Nanotubes: Pore Structure Evaluation of Anodized Alumina Templated Carbon Nanotube Membranes Through Adsorption and Permeability Studies. Advanced Functional Materials, 2010, 20, 2500-2510.	14.9	26
117	Evaluation of laser cleaning of ancient Greek, Roman and Byzantine coins. Surface and Interface Analysis, 2010, 42, 671-674.	1.8	6
118	Tuning the lateral density of ZnO nanowire arrays and its application as physical templates for radial nanowire heterostructures. Journal of Materials Chemistry, 2010, 20, 3848.	6.7	27
119	Chemical Synthesis and Self-Assembly of Hollow Ni/Ni ₂ P Hybrid Nanospheres. Journal of Physical Chemistry C, 2010, 114, 7582-7585.	3.1	50
120	Enhanced magnetic properties of FePt nanoparticles codeposited on Ag nanoislands. Journal of Applied Physics, 2009, 105, 093914.	2.5	5
121	Zinc and oxygen vacancies in ZnO nanorods. Journal of Applied Physics, 2009, 106, .	2.5	46
122	Synthesis and Magnetic Properties of Fe3O4 Nanoparticles Coated with Biocompatible Double Hydrophilic Block Copolymer. Journal of Nanoscience and Nanotechnology, 2009, 9, 4753-4759.	0.9	8
123	Comparative evaluation of ultrafast laser beam interaction with the silvering in late Roman coins. Proceedings of SPIE, 2009, , .	0.8	1
124	Gummic acid stabilized Î ³ -Fe2O3 aqueous suspensions for biomedical applications. Hyperfine Interactions, 2009, 190, 59-66.	0.5	3
125	PL study of oxygen defect formation in ZnO nanorods. Microelectronics Journal, 2009, 40, 296-298.	2.0	110
126	Removal of Reactive Red 195 from aqueous solutions by adsorption on the surface of TiO2 nanoparticles. Journal of Hazardous Materials, 2009, 170, 836-844.	12.4	156

#	Article	IF	CITATIONS
127	Photocatalytic synthesis of Se nanoparticles using polyoxometalates. Catalysis Today, 2009, 144, 2-6.	4.4	28
128	Development of a Ce–Zr–La modified Pt/γ-Al2O3 TWCs' washcoat: Effect of synthesis procedure on catalytic behaviour and thermal durability. Applied Catalysis B: Environmental, 2009, 90, 162-174.	20.2	105
129	Study of hybrid solar cells made of multilayer nanocrystalline titania and poly(3-octylthiophene) or poly-(3-(2-methylhex-2-yl)-oxy-carbonyldithiophene). Nanotechnology, 2009, 20, 495201.	2.6	26
130	Homogeneous core/shell ZnO/ZnMgO quantum well heterostructures on vertical ZnO nanowires. Nanotechnology, 2009, 20, 305701.	2.6	44
131	Polypyrrole/MWNT nanocomposites synthesized through interfacial polymerization. Synthetic Metals, 2009, 159, 632-636.	3.9	48
132	Effect of the conditions of platinum deposition on titania nanocrystalline films on the efficiency of photocatalytic oxidation of ethanol and production of hydrogen. Photochemical and Photobiological Sciences, 2009, 8, 639-643.	2.9	25
133	Zinc oxide nanorod based photonic devices: recent progress in growth, light emitting diodes and lasers. Nanotechnology, 2009, 20, 332001.	2.6	572
134	Optically Active Spherical Polyelectrolyte Brushes with a Nanocrystalline Magnetic Core. Advanced Functional Materials, 2008, 18, 1694-1706.	14.9	23
135	Synthesis and characterisation of carbon nanotube modified anodised alumina membranes. Microporous and Mesoporous Materials, 2008, 110, 25-36.	4.4	30
136	Structural, thermal, electrical and magnetic properties of Eurofer 97 steel. Journal of Nuclear Materials, 2008, 373, 1-8.	2.7	122
137	Growth and Characterization of ZnO Nano- and Microstructures. , 2008, , 293-323.		3
138	No Aging Phenomena in Ferrofluids: The Influence of Coating on Interparticle Interactions of Maghemite Nanoparticles. ACS Nano, 2008, 2, 977-983.	14.6	24
139	Ultraviolet femtosecond, picosecond and nanosecond laser microstructuring of silicon: structural and optical properties. Applied Optics, 2008, 47, 1846.	2.1	70
140	Some Physicochemical Aspects of Nanoparticulate Magnetic Iron Oxide Colloids in Neat Water and in the Presence of Poly(vinyl alcohol). Langmuir, 2008, 24, 11489-11496.	3.5	25
141	A General Chemical Route for the Synthesis of Capped Nanocrystalline Materials. Journal of Nanoscience and Nanotechnology, 2008, 8, 3117-3122.	0.9	19
142	Spatial fluctuations of optical emission from single ZnO/MgZnO nanowire quantum wells. Nanotechnology, 2008, 19, 115202.	2.6	37
143	Engineering of FePt nanoparticles by e-beam co-evaporation. Nanotechnology, 2008, 19, 135702.	2.6	7
144	Synthesis and Characterization of Iron Oxide Nanoparticles Encapsulated in Lipid Membranes. Journal of Biomedical Nanotechnology, 2008, 4, 313-318.	1.1	5

#	Article	IF	CITATIONS
145	Growth Evolution and Characterization of PLD Zn(Mg)O Nanowire Arrays. , 2008, , 113-125.		3
146	Experimental study on the use of laser cleaning of silver plating layers in Roman coins. , 2008, , 309-315.		0
147	Low temperature growth of single-crystal ZnO nanorods. Nanotechnology, 2007, 18, 275601.	2.6	9
148	Large-Scale Synthesis, Size Control, and Anisotropic Growth of <i>γ</i> -Fe ₂ O ₃ Nanoparticles: Organosols and Hydrosols. Journal of Nanoscience and Nanotechnology, 2007, 7, 2753-2757.	0.9	19
149	Materials and electrical characterization of molecular beam deposited CeO2 and CeO2/HfO2 bilayers on germanium. Journal of Applied Physics, 2007, 102, .	2.5	48
150	<title>Experimental study on the effect of wavelength and fluence in the laser cleaning of silvering
in late Roman coins (Mid 3rd/4th century AD)</title> . , 2007, , .		3
151	Direct Chemical Synthesis of L10FePt Nanostructures. Chemistry of Materials, 2007, 19, 1898-1900.	6.7	24
152	Synthesis and self-organization of Au nanoparticles. Nanotechnology, 2007, 18, 485604.	2.6	34
153	Biopolymer Networks for the Solid-State Production of Porous Magnetic Beads and Wires. Advanced Functional Materials, 2007, 17, 1409-1416.	14.9	8
154	Fabrication of ZnO nanorod-based p–n heterojunction on SiC substrate. Superlattices and Microstructures, 2007, 42, 415-420.	3.1	26
155	Growth and optical study of ZnO nanorods. Superlattices and Microstructures, 2007, 42, 431-437.	3.1	9
156	Silicone-functionalized carbon nanotubes for the production of new carbon-based fluids. Carbon, 2007, 45, 1583-1585.	10.3	46
157	Ordering kinetics of chemically synthesized FePt nanoparticles. Journal of Magnetism and Magnetic Materials, 2007, 316, e169-e172.	2.3	10
158	<i>In vitro</i> studies on ultrasmall superparamagnetic iron oxide nanoparticles coated with gummic acid for T2 MRI contrast agent. Biomicrofluidics, 2007, 1, 44104.	2.4	14
159	Growth of ZnO nanorods by a simple chemical method. Applied Physics A: Materials Science and Processing, 2007, 88, 35-39.	2.3	28
160	Structural and photoluminescence properties of ZnO nanoparticles on silicon oxide. Applied Physics A: Materials Science and Processing, 2007, 88, 41-44.	2.3	5
161	Selective growth of ZnO nanorods in aqueous solution. Superlattices and Microstructures, 2007, 42, 425-430.	3.1	23
162	Self-Organization of Four Symmetric Tri-phenyl-benzene Derivatives. Crystal Growth and Design, 2006, 6, 2486-2492.	3.0	24

#	Article	IF	CITATIONS
163	Chemical synthesis and characterization of hcp Ni nanoparticles. Nanotechnology, 2006, 17, 3750-3755.	2.6	117
164	Simple method for the fabrication of a high dielectric constant metal-oxide-semiconductor capacitor embedded with Pt nanoparticles. Applied Physics Letters, 2006, 88, 073106.	3.3	29
165	Functionalized Carbon Nanotubes: Synthesis of Meltable and Amphiphilic Derivatives. Small, 2006, 2, 1188-1191.	10.0	72
166	Zinc oxide nanoparticles on silicon. Superlattices and Microstructures, 2006, 39, 115-123.	3.1	7
167	The effect of Mn doping in FePt nanoparticles on the magnetic properties of the L10phase. Nanotechnology, 2006, 17, 4270-4273.	2.6	19
168	Structural Study of Very Thin Anodic Alumina Films on Silicon by Anodization in Citric Acid Aqueous Solution. Journal of Nanoscience and Nanotechnology, 2005, 5, 454-495.	0.9	3
169	Self-assembled zinc oxide nanodots on silicon oxide. Journal of Physics: Conference Series, 2005, 10, 121-124.	0.4	4
170	HfO2 high-κ gate dielectrics on Ge (100) by atomic oxygen beam deposition. Applied Physics Letters, 2005, 86, 032908.	3.3	144
171	Synthesis and Characterization of 3D CoPt Nanostructures. Journal of the American Chemical Society, 2005, 127, 13756-13757.	13.7	107
172	Nanotemplate alumina films on a silicon substrate fabricated by electrochemistry. Journal of Physics: Conference Series, 2005, 10, 159-162.	0.4	3
173	EELS study of oxygen superstructure in epitaxial Y2O3 layers. Materials Science and Engineering B: Solid-State Materials for Advanced Technology, 2004, 109, 52-55.	3.5	8
174	Materials design data for reduced activation martensitic steel type EUROFER. Journal of Nuclear Materials, 2004, 329-333, 257-262.	2.7	118
175	Growth of rare earth silicides on silicon. Journal of Physics and Chemistry of Solids, 2003, 64, 87-93.	4.0	15
176	Oxygen vacancy ordering in epitaxial layers of yttrium oxide on Si (001). Applied Physics Letters, 2003, 82, 4053-4055.	3.3	53
177	Magnetite and Co ferrite- based clay composites. Clay Minerals, 2002, 37, 135-141.	0.6	11
178	Epitaxial erbium silicide on Ge+ implanted silicon. Nuclear Instruments & Methods in Physics Research B, 2002, 196, 174-179.	1.4	3
179	Exchange Resins in shape Fabrication of Hollow Inorganic and Carbonaceous-Inorganic Composite Spheres. Advanced Materials, 2002, 14, 21-24.	21.0	36
180	Epitaxial ErSi2â^'x on strained and relaxed Si1â^'xCex. Materials Science and Engineering B: Solid-State Materials for Advanced Technology, 2002, 89, 382-385.	3.5	4

#	Article	IF	CITATIONS
181	Growth and electrical characterisation of highly doped p-SiGe/Si heterostructures. Materials Science and Engineering B: Solid-State Materials for Advanced Technology, 2002, 89, 221-224.	3.5	0
182	Surface morphology of low temperature grown GaAs on singular and vicinal substrates. Materials Science and Engineering B: Solid-State Materials for Advanced Technology, 2002, 88, 205-208.	3.5	6
183	Increased epitaxial thickness limit in low-temperature GaAs grown on a vicinal substrate. Physica E: Low-Dimensional Systems and Nanostructures, 2002, 13, 1190-1194.	2.7	5
184	Catalytic synthesis of carbon nanotubes on clay minerals. Carbon, 2002, 40, 2641-2646.	10.3	121
185	Magnetic Modification of the External Surfaces in the MCM-41 Porous Silica:Â Synthesis, Characterization, and Functionalization. Journal of Physical Chemistry B, 2001, 105, 7432-7437.	2.6	83
186	Aqueous polymerization of protonated 4-vinylpyridine in montmorillonite. Applied Clay Science, 2001, 19, 77-88.	5.2	15
187	Epitaxial dysprosium silicide films on silicon: growth, structure and electrical properties. Thin Solid Films, 2001, 397, 138-142.	1.8	12
188	Low-temperature transport properties of quasi-crystalline Al86Mn14 thin films. Physica B: Condensed Matter, 2001, 296, 275-279.	2.7	0
189	Synthesis, and structural and morphological characterization of iron oxide-ion-exchange resin and -cellulose nanocomposites. Applied Organometallic Chemistry, 2001, 15, 414-420.	3.5	20
190	Chemical and X-Ray Diffraction Peak Broadening Analysis, Electron Microscopy and IR Studies of Biological Apatites. Materials Science Forum, 2001, 378-381, 759-764.	0.3	6
191	Extending the epitaxial thickness limit in low-substrate-temperature- grown GaAs. Applied Physics Letters, 2001, 79, 3422-3424.	3.3	2
192	Direct heteroepitaxy of crystalline Y2O3 on Si (001) for high-k gate dielectric applications. Journal of Applied Physics, 2001, 90, 4224-4230.	2.5	62
193	Transmission electron microscopy and X-ray diffraction study of T1and Ω precipitates in Al—Li alloys. Philosophical Magazine A: Physics of Condensed Matter, Structure, Defects and Mechanical Properties, 2000, 80, 1055-1063.	0.6	3
194	The size distribution of metal clusters produced in plasma-discharge hollow-cathode source. Scripta Materialia, 1999, 12, 311-314.	0.5	3
195	CW and Pulsed EPR Study of Silver Nanoparticles in a SiO2 Matrix. Journal of Sol-Gel Science and Technology, 1998, 13, 503-508.	2.4	34
196	The effect of Ag additions on the microstructure of aluminium–lithium alloys. Journal of Materials Science, 1998, 33, 4015-4020.	3.7	5
197	Low-field Hall coefficient of Al-4d dilute alloys: The role of the anisotropic impurity scattering. Solid State Communications, 1998, 106, 405-408.	1.9	0
198	Microstructure of AlLiCuMgZr alloys with In additions. Materials Science & Engineering A: Structural Materials: Properties, Microstructure and Processing, 1998, 256, 280-288.	5.6	8

#	Article	IF	CITATIONS
199	Size distribution and EPR of silver nanoparticles in SiO2 matrix. Journal of Non-Crystalline Solids, 1998, 224, 17-22.	3.1	30
200	Microstructural modification in Co/Cu giant-magnetoresistance multilayers. Journal of Applied Physics, 1998, 83, 3724-3730.	2.5	24
201	Growth, structure and electrical properties of epitaxial thulium silicide thin films on silicon. Journal of Applied Physics, 1997, 81, 1217-1221.	2.5	6
202	Size selection by cluster deflection in an electric field. Scripta Materialia, 1997, 8, 771-784.	0.5	3
203	The influence of Î ⁴ precipitates on the electrical resistivity and low-field Hall coefficient of Al-Li alloys. The Philosophical Magazine: Physics of Condensed Matter B, Statistical Mechanics, Electronic, Optical and Magnetic Properties, 1994, 70, 67-75.	0.6	2
204	Deviations from Mathiessen's rule for dilute Al-Li alloys. Physical Review B, 1993, 47, 13147-13150.	3.2	3
205	Strong anisotropic electron-impurity scattering in diluteAlLi alloys. Physical Review B, 1992, 46, 4508-4510.	3.2	5
206	The Hall coefficient of Yb alloys. Physica B: Condensed Matter, 1991, 172, 405-408.	2.7	2
207	Hall Coefficient of Dilute CuPd, CuRh, CuZr, and CuY Alloys dâ€Resonance Scattering. Physica Status Solidi (B): Basic Research, 1990, 157, 351-356.	1.5	1